Published in final edited form as:
Dev Cell. 2011 September 13; 21(3): 469–478. doi:10.1016/j.devcel.2011.08.008.

The Permeability Transition Pore Controls Cardiac Mitochondrial Maturation and Myocyte Differentiation

Jennifer R. Hom[1,8], **Rodrigo A. Quintanilla**[2,8], **David L. Hoffman**[1], **de Mesy Bentley Karen L.**[5], **Jeffery D. Molkentin**[6], **Shey-Shing Sheu**[3,7], and **George A. Porter**[1,3,4,*]

[1]Department of Pediatrics Division of Cardiology, University of Rochester School of Medicine and Dentistry, Rochester, NY 14642, USA

[2]Department of Anesthesiology, University of Rochester School of Medicine and Dentistry, Rochester, NY 14642, USA

[3]Department of Pharmacology and Physiology, University of Rochester School of Medicine and Dentistry, Rochester, NY 14642, USA

[4]Aab Cardiovascular Research Institute, University of Rochester School of Medicine and Dentistry, Rochester, NY 14642, USA

[5]Pathology & Laboratory Medicine and the Electron Microscope Research Core, University of Rochester School of Medicine and Dentistry, Rochester, NY 14642, USA

[6]Department of Molecular Cardiovascular Biology, Cincinnati Children's Hospital Medical Center and Howard Hughes Medical Institute, Cincinnati, OH 45229, USA

[7]Center for Translational Medicine, Thomas Jefferson University, Philadelphia, PA 19107, USA

SUMMARY

Although mature myocytes rely on mitochondria as the primary source of energy, the role of mitochondria in the developing heart is not well known. Here, we find closure of the mitochondrial permeability transition pore (mPTP) drives maturation of mitochondrial structure and function and myocyte differentiation. Cardiomyocytes at embryonic day (E) 9.5, when compared to E13.5, displayed fragmented mitochondria with few cristae, a less polarized mitochondrial membrane potential, higher reactive oxygen species (ROS) levels, and an open mPTP. Pharmacologic and genetic closing of the mPTP yielded maturation of mitochondrial structure and function, lowered ROS, and increased myocyte differentiation (measured by counting Z-bands). Furthermore, myocyte differentiation was inhibited and enhanced with oxidant and antioxidant treatment, respectively, suggesting that redox signaling pathways lie downstream of mitochondria to regulate cardiac myocyte differentiation.

[*]**Corresponding author:** George A. Porter, Jr., MD, PhD, Assistant Professor, University of Rochester Medical Center, Department of Pediatrics, Division of Cardiology, 601 Elmwood Ave. Box 631, Rochester, NY 14642, george_porter@urmc.rochester.edu, Phone: (585) 276-4769, Fax: (585) 275-7436.
[8]These authors contributed equally to this work

INTRODUCTION

The heart is the first functional organ to form in the embryo, beginning at about embryonic day (E) 8 in the mouse, becoming a looped tube by E9.5, and resulting in a fully septated heart at around E13.5. Embryos can survive with abnormally formed hearts; however, they cannot survive if the heart does not function well enough to provide effective circulation (Conway et al., 2003). Despite the recent advances in cardiac developmental biology, in many cases the exact causes of embryonic cardiac failure are not well understood. A few studies demonstrated that mitochondria are important to the development of the heart, as dysfunction of the mitochondrial electron transport chain (ETC) can cause heart malformation and embryonic death between E8.5 and E10.5, suggesting that mitochondrial function is essential to cardiac function and survival of the embryo (Ingraham et al., 2009; Larsson et al., 1998).

Mitochondria in the adult heart are well characterized and occupy over 30% of the cell volume. It is thought that complex mitochondrial networks exist within the adult heart myocyte for the transmission of substrates and ATP to the inner parts of the cell by diffusion through connected, filamentous mitochondria (Skulachev, 2001). Generally, mitochondrial morphology in mature cells correlates with mitochondrial function, as changes in mitochondrial fusion or fission require the pinching off or fusing of both the outer and inner mitochondrial membranes, thereby affecting cristae morphology and the diffusion of ADP (Mannella, 2006). In contrast, much less is known about mitochondria and bioenergetics in the developing heart (reviewed in Porter et al., 2011). Mitochondria in pre-implantation embryos undergo cyclic changes in their inner mitochondrial membrane (IMM) structure. During the blastocyst stage, the IMM is less complex compared to earlier or later stages (Dumollard et al., 2009). A few studies demonstrate that, as the heart establishes placental-embryonic circulation, the cardiac mitochondria mature, and similar changes are seen during cardiac stem cell differentiation (Chung et al., 2007; Krishnan et al., 2008; Shepard et al., 1998). However, the transition from immature mitochondrial structure and function in early myocytes to a mature mitochondrial network in the adult myocyte has not been investigated in detail.

In this study, we examined the relatively unexplored role of mitochondrial biology in the embryonic heart. We found that the mitochondrial permeability transition pore (mPTP) is open in the early heart and that closure of this mPTP led to dramatic maturation of mitochondrial structure and function, which accelerated myocyte differentiation. We modulated mPTP opening using pharmacological agents that affect the adenine nucleoside translocase (ANT), a potential component of the mPTP, and Cyclophilin D (CyP-D), a mitochondrial matrix peptidyl-prolyl *cis-trans* isomerase that is known to regulate mPTP opening (Baines and Molkentin, 2009; Brookes et al., 2004; Crompton, 1999; Gunter and Sheu, 2009; Halestrap, 2009; Lemasters et al., 2009), or genetic deletion of the *Ppif* gene that encodes CyP-D (Baines et al., 2005; Elrod et al., 2010). Although mPTP opening is generally associated with apoptosis, our findings indicate that mPTP opening in early embryonic heart is non-pathologic. In addition, mPTP closure quickly decreased intracellular ROS levels, and treatment with exogenous oxidants and antioxidants also regulated myocyte differentiation, irrespective of the state of the mPTP. Our findings suggest a critical role of the embryonic mPTP as a mediator of mitochondrial maturation and cardiac differentiation via redox signaling and suggest that the mPTP and oxidative state may be targets to modulate cardiac development and function in the embryo and fetus and to enhance cardiac myocyte differentiation for cardiac regeneration.

RESULTS

Mitochondrial morphology, ultrastructure, and mass change during embryonic cardiac development

We examined mitochondrial morphology using epifluorescence and confocal microscopy in cultured ventricular myocytes from C57BL/6N mice loaded with MitoTracker green (MTG). At E9.5, mitochondria were fragmented, round and dilated, while at E13.5, mitochondria were more elongated and branched, forming thin, filamentous, interconnected networks (Figures 1A and C, 2A and B, and 4A). Cellular organization also changed; whereas the E9.5 mitochondria were frequently clustered around the nucleus with little association with the immature contractile apparatus, the E13.5 mitochondria were arranged more in a linear pattern spanning the length of the cell and between the developing contractile filaments (Figures 1A–1C and 4A). Statistical analysis revealed that mitochondrial length, network complexity, and area increased during the embryonic period (Figures 1D and S1A–D).

Electron microscopy (EM) of whole embryo hearts was performed to examine details of mitochondrial ultrastructure. At each developmental stage, mitochondria were classified based on the arrangement of the cristae and the matrix. The mitochondria were divided into four classes: Class 1 is “very immature” and has rare or no cristae and an expanded matrix; Class 2 is “immature” and has sparse, tubular cristae with a few tubular cristae connections to the periphery and a slightly expanded matrix; Class 3 is “almost mature” and has many and better defined cristae and many tubular cristae connections to the periphery, but a mostly compacted matrix and occasional matrix translucence/“voids;” and Class 4 is “mature” and has abundant, organized/laminar cristae with multiple tubular connections to the periphery and a compacted matrix with no voids (Figure S1E). As demonstrated in Figure 1E, mitochondria from E9.5 hearts tended to have immature cristae compared to those from older embryos, and quantification confirmed a progressive and statistically significant increase in mitochondrial class distribution as the hearts developed, suggesting a “maturation” of mitochondrial ultrastructure (Figure 1F).

In addition, Western blot analysis revealed that the expression of the mitochondrial proteins ANT1, the complex II 75 kDa subunit, and cyclophilin D (CyP-D) increased during development (Figure S2A), indicating that E9.5 hearts contained a reduced mitochondrial population compared to older ages. These observations were corroborated with imaging experiments, in which myocytes from different ages were loaded with MTG and mitochondrial mass was measured (Figure S1C).

Mitochondrial function changes as the embryonic heart ages

Next, we examined mitochondrial function in cultured myocytes by measuring mitochondrial membrane potential ($\Delta\psi_m$) and ROS levels. To compare $\Delta\psi_m$ between specimens, the ratio was taken of tetramethylrhodamine methyl ester (TMRE) to MTG intensity, whose retention in the mitochondria is and is not dependent on $\Delta\psi_m$, respectively (Quintanilla et al., 2008). $\Delta\psi_m$ increased in cultured cardiac myocytes as the embryo aged (Figure 2A and C), indicating that mitochondrial function matures in coordination with mitochondrial network maturation and cardiac organogenesis.

To test ETC function during the embryonic period, $\Delta\psi_m$ was measured upon addition of different combinations of ETC inhibitors (Figure 2E and F). First, oligomycin did not cause a drop in $\Delta\psi_m$ at any of the ages, indicating that complex V does not maintain the $\Delta\psi_m$ by the hydrolysis of ATP. In contrast, the complex II inhibitor, malonate, decreased TMRE fluorescence in E9.5 myocytes more than in E13.5 myocytes, while rotenone decreased TMRE fluorescence in E13.5 myocytes but had no effect on E9.5 myocytes. These data

suggest that at E9.5, complex II is the primary entry point of electrons into the ETC, and that by E13.5 complex I becomes important.

Myocyte ROS levels fell during the embryonic period when assayed using 2'-7'-dichlorofluorescin diacetate (DCF) (Quintanilla et al, 2009). ROS levels were high throughout the entire cell in E9.5 myocytes and decreased in the older ages (Figure 2B and D). MitoTracker Red (MTR) was loaded simultaneously with DCF and revealed that DCF fluorescence localized to the mitochondria in the later ages (Figure 2B). DCF fluorescence did not change in the presence of the metal chelator, diethylenetriaminepentaacetic acid (DTPA, not shown), confirming that the DCF signal is due to changes in ROS levels and not to changes in free iron levels (Tampo et al., 2003).

Mitochondrial morphology and function changes in embryonic cardiac myocytes upon closure of the mPTP

The changes in mitochondrial structure and function we observed suggest that early myocytes could have an open mPTP, which has been associated with collapse of $\Delta\psi_m$, complex I deficiency, and changes in free radical levels (Brookes et al., 2004; Crompton, 1999; Fontaine et al., 1998; Gunter and Sheu, 2009; Halestrap, 2009; Lemasters et al., 2009). Generally, mPTP opening is thought to be a pathologic condition that initiates apoptosis. However, the apoptotic factors cytochrome *c* (cyt *c*) and apoptosis inducing factor (AIF) localized within the mitochondria and were not released into the cytosol in E9.5 myocytes, indicating that pathologic opening of the embryonic mPTP did not occur in these early myocytes (Figures 1B and C, 4A, and S3B), which agrees with previous data that demonstrate virtually no apoptosis occurs in the early embryonic heart (Poelmann et al., 2000).

The absence of mPTP-initiated apoptosis does not preclude non-pathologic and/or transient mPTP opening, as has been suggested in some reports (Hausenloy et al., 2010; Wang et al., 2008). The mPTP is defined by its inhibition by Cyclosporin A (CsA), an immunosuppressant that binds to mitochondrial CyP-D to block the calcium ion-induced permeability transition (Basso et al, 2005; Friberg et al, 1998). Opening of the mPTP causes the IMM to become permeable and leads to free movement of ions and dissipation of the $\Delta\psi_m$ (Baines and Molkentin, 2009; Brookes et al., 2004; Crompton, 1999; Gunter and Sheu, 2009; Halestrap, 2009; Lemasters et al., 2009). To determine if the mPTP was open in E9.5 myocytes, we used the cobalt/calcein AM quenching method (Petronilli et al, 1999). In untreated E9.5 myocytes, cobalt quenched calcein fluorescence throughout the cell and in mitochondria due to free movement of these molecules through an open mPTP. However, when cultures of E9.5 myocytes were treated with 500 nM CsA for 2 hours, mitochondrial calcein fluorescence increased, indicating that CsA closed the mPTP, preventing cobalt entry (Figure 3E).

More importantly, treatment with CsA for 2 hours increased mitochondrial length and $\Delta\psi_m$ and decreased ROS levels (Figure 3) in E9.5 myocytes. In contrast, at E11.5 and 13.5, CsA did not significantly change mitochondrial length, $\Delta\psi_m$, or ROS levels (Figure S2C–E) compared to age-matched WT controls. In addition to blocking mPTP opening, CsA also inhibits the phosphatase calcineurin. Therefore, to determine if the calcineurin pathway was involved in these changes, we treated cells with FK-506, which blocks calcineurin activity via its receptor FKBP12, yet has no effect on the mPTP (Friberg et al, 1998). Treatment with 500 nM FK-506 for 2 hours had no effects on any of the parameters tested above at any of the ages (Figures 3 and S2C–E), suggesting the CsA effects were specific to inhibition of the mPTP.

The mPTP is regulated by CyP-D expression and function (Baines and Molkentin, 2009; Brookes et al., 2004; Crompton, 1999; Gunter and Sheu, 2009; Halestrap, 2009; Lemasters et al., 2009), and CyP-D is expressed in the embryonic heart (Figure S2A). Thus, we examined myocytes from CyP-D null mice, in which mPTP is resistant to opening (Baines et al., 2005; Elrod et al., 2010). Although embryonic and cardiac morphology of the CyP-D null embryos was generally normal, we have found a number of E9.5 and 11.5 litters with a wider range of apparent embryonic age than is usually seen in wild-type litters. For example, one recent E11.5 litter contained embryos ranging from E8.75 to E11.5; two E10.5 embryos were dead and the E8.75 embryo contained an abnormal heart with a bulbous left ventricle and a thin outflow tract (not shown). Many mitochondria from E9.5 CyP-D null hearts displayed almost mature cristae, and quantification showed that the ultrastructure of E9.5 CyP-D mitochondria was not significantly different from those in either WT E9.5 or 11.5 myocytes, suggesting that the maturation of these mitochondria lay somewhere in between (Figures 3C and D). In addition, cultured E9.5 CyP-D null myocytes had significantly increased mitochondrial length and $\Delta\psi_m$ and lower ROS levels compared to WT E9.5 controls (Figure 3). In contrast, cultured E11.5 and 13.5 CyP-D null myocytes showed no significant differences in these parameters compared to WT controls (Figure S2C–E). These results further suggest that the mPTP is open in WT E9.5 myocytes and that its closure in later ages improves mitochondrial function in the developing heart.

Closure of the mPTP enhances myocyte differentiation

CsA has been shown to enhance cardiac myocyte differentiation from embryonic stem cells in a calcineurin and NFAT-independent manner (Yan et al., 2009). To determine if the mPTP plays a role in myocyte differentiation in the embryo, the Z-bands of cultured cardiac myocytes were labeled for the striated muscle isoform of sarcomeric α-actinin (Borisov et al., 2008). The number of myocyte Z-bands increased in WT myocytes during the embryonic period, validating this assay as a measure of differentiation (Figures 4, 6, and S2F). Closure of the mPTP at E9.5, by treating cultures with CsA for 24 hours or examining CyP-D null myocytes, caused a significant increase in the number of Z-bands compared to E9.5 WT controls (Figure 4). In contrast, these effects on differentiation were not seen in E11.5 and 13.5 myocytes (Figure S2F). As above, the effects of CsA on myocyte differentiation were likely not due to its inhibition of calcineurin, as FK-506 did not alter the number of Z-bands in E9.5 WT myocytes (Figure 4), and treatment of CyP-D null myocytes with either CsA or FK-506 had no effect (not shown).

Electron micrographs of E9.5 and 11.5 WT and CyP-D hearts demonstrated similar changes in differentiation *in vivo* (Figure 5). E9.5 (25–26 somites) WT hearts were only 2–3 cell layers thick and composed of myocytes and an inner layer of endocardial cells. The myocytes contain few, relatively immature myofibrils that spanned the cell generally perpendicular to the long axis of the heart tube. In contrast, E9.5, somite-matched CyP-D hearts had more cell layers with evidence of early trabeculation, and the cells had more myofibrils, which tended to appear more organized compared to WT cells. As with the *in vitro* data, by E11.5 these differences were not apparent. In both WT and CyP-D null hearts, myocytes in the compact myocardium (the wall) contained few myofibrils, although more were seen in cells near the ventricular lumen, while the trabeculae of both genotypes were more differentiated and contained more myofibrils, as expected (Porter et al., 2011).

To confirm the importance of mPTP closure and to determine the effects of its sustained opening, we treated cultures with the ANT antagonist, bongkrekic acid (BKA), and agonist, carboxyatractyloside (CAT), which close and open the mPTP, respectively. These agents had the expected effects on mPTP activity in calcein quenching experiments (Figure S2B). Treating WT E9.5 myocytes with BKA increased the number of Z-bands compared to controls, yet had no effect on E13.5 myocytes (Figure 6). In contrast, opening of the mPTP

with CAT for 24 hours inhibited Z-band formation in E13.5 myocytes but had no effect on E9.5 myocytes (Figure 6). These data further suggest that closure of the mPTP after E9.5 may control myocyte differentiation.

Changes in ROS levels lie downstream of mPTP closure to regulate myocyte differentiation

The experiments presented above demonstrated that closure of the mPTP is associated with (Figure 2B and D) or may lead to (Figure 3G) a decrease in ROS levels in embryonic myocytes. Alternatively, ROS are known to stimulate mPTP opening. Therefore, we tested whether the mPTP lies upstream of redox signaling to affect the differentiation of cultured E9.5 myocytes. Specimens were treated with 6-Hydroxy-2,5,7,8-tetramethylchroman-2-carboxylic acid (Trolox), an anti-oxidant, or *tert*-butyl hydroperoxide (tBHP), a stable oxidant, for 24 hours. Trolox alone or with concurrent CAT treatment enhanced differentiation, while tBHP alone or concurrent with BKA treatment inhibited differentiation (Figure 6). These data suggest that early myocyte differentiation is regulated by changes in ROS levels and that this mechanism lies downstream of mPTP closure.

DISCUSSION

Several studies have shown the importance of mitochondria and mPTP activity in cardioprotection and the pathophysiology of cardiomyopathies (Baines et al., 2005; Burelle et al., 2010). However, the role of mitochondrial biology in the developing heart is poorly understood, although a few reports indicate that mitochondria regulate cardiac stem cell and skeletal myocyte differentiation (Chung et al., 2007; De Palma et al., 2010; Yan et al., 2009). Our results not only characterize the development of mitochondrial structure and function during embryonic cardiac myocyte differentiation, but further demonstrate that the mPTP lies upstream of changes in mitochondrial morphology, mitochondrial function, and myocyte differentiation. These results highlight changes in two mechanisms by which the mPTP may regulate cardiac myocyte differentiation: bioenergetics and redox signaling.

First, changes in mPTP activity may affect myocyte bioenergetics to regulate myocyte differentiation. In the developing heart, cardiac energetic demands must increase dramatically to match increasing cardiac performance required by embryonic growth (Conway et al., 2003; Porter et al, 2011), and closure of the mPTP may quickly increase ATP production by increasing the coupling of the electron transport chain and ATP synthase. In addition, Elrod and colleagues recently demonstrated that mitochondria from CyP-D null hearts maintain approximately 2-fold higher calcium content at baseline, resulting in greater mitochondrial activity and enhanced glucose utilization (Elrod et al., 2010). Similar control of calcium levels in the mitochondrial matrix in the embryonic heart may account, in part, for the changes in ETC activity we observed during embryonic cardiac development and may result in increased ATP production. Finally, intrinsic changes in ETC complex composition and activity, such as we observed for complex I, may play a role in this process. Therefore, we propose that as the mPTP closes, mitochondrial function increases, and an increase in ATP production may allow myocytes to differentiate to a stage in which they are able to provide the contractile force needed to ensure adequate circulation and embryonic survival.

Second, our results suggest that mPTP activity regulates cellular redox signaling during myocyte differentiation, and, although the mechanisms by which mPTP regulates ROS remain to be determined, we speculate that complex I is involved, as it is a major source of mitochondrial ROS. We found that E9.5 myocytes were highly oxidized, but closure of the mPTP decreased ROS levels and enhanced myocyte differentiation. Antioxidant treatment also enhanced differentiation of E9.5 myocytes, while oxidant treatment significantly

inhibited differentiation in both E9.5 and 13.5 myocytes. These data suggest a link between the mPTP, redox signaling, and myocyte differentiation, which we tested by combining agents that affected the mPTP and oxidative state. Upon treatment of E9.5 myocytes with the antioxidant concurrent with the mPTP-inducing CAT treatment, myocyte differentiation remained enhanced. In contrast, when E9.5 myocytes were treated with oxidant concurrent with the mPTP-closing BKA treatment, myocyte differentiation remained inhibited. Together, these observations suggest that the control of ROS levels could be a mechanism by which the mPTP regulates differentiation between E9.5 and 11.5. Consistent with this idea are recent studies, which show that embryonic stem cells also rely on redox signaling during differentiation into cardiac myocytes (Buggisch et al., 2007).

Opening of the mPTP in the early embryonic heart may play a protective role

According to the data presented in Krishnan (2008), between E8.5 and 10 the pO_2 in the mouse heart is lower than 10 mmHg. It is likely that this is lower than what is observed in the rest of the embryo at that age due both to a lack of effective placental circulation and increased energy requirements of the heart, which has begun to beat and circulate blood. After E10, the pO_2 of the heart is higher due to the initiation of effective placental circulation. Therefore, major changes occur in the physiology of the heart between E9.5 and 11.5 as oxygen supply and energy demands increase.

The purpose of this mPTP-mediated delay of differentiation in early development may be, in part, to compensate for physiological changes that have yet to occur. The increase in energy demands likely requires dramatic maturation of mitochondrial function. However, the low oxygen supply at E9.5 may inhibit this maturation; e.g., these very immature myocytes have few mitochondria with immature mitochondrial structure and function as well as high oxidative stress, despite the low oxygen tension. This paradoxically high oxidative stress may be due to an immature ETC, decreased anti-oxidant defenses that are controlled by mitochondria (Aon et al., 2010), or a yet undetermined mechanism. We hypothesize that the high ROS levels and low ATP production from immature mitochondria may prevent further myocyte differentiation in order to protect the heart during this period of low oxygen supply. Yet, as the placental circulation is established and oxygen supply increases, mitochondria mature, leading to decreased oxidative stress and increased ATP production. This maturation allows myocytes to differentiate directly via redox signaling and indirectly by increasing available energy, as discussed above.

If this is the case, then changes in the function of the mPTP may cause abnormal differentiation of cardiac myocytes and disrupt cardiac morphogenesis. Although it was initially reported that CyP-D null mice have no cardiac phenotype and survive gestation and have a normal lifespan (Baines et al., 2005; Basso et al., 2005; Nakagawa et al., 2005), we observed “premature” mitochondrial maturation and myocyte differentiation in E9.5 CyP-D null myocytes compared to wild-type controls. In contrast we found that myocytes from older CyP-D null hearts were indistinguishable from their WT controls suggesting a critical period between E9.5 and 11.5 for mPTP closure that may not necessarily be pathologic. However, the abnormal variation in developmental stages in occasional litters of CyP-D mice we have observed may also indicate subtle pathology in the early embryo. Moreover, a recent paper shows that CyP-D mice do have abnormal cardiac physiology, particularly when placed under stress (Elrod et al., 2010). Therefore, deletion of CyP-D may not be a completely benign.

In contrast, although deletion of CyP-D and closure of the mPTP, with the resulting mild acceleration of cardiac myocyte differentiation, is generally tolerated, we postulate that the converse phenomenon, sustained opening of the mPTP, would be much more devastating. If this were to occur, then mitochondrial maturation and myocyte differentiation would be

inhibited leading to an inability of the developing heart to meet the demands of the growing embryo. Future experiments that manipulate mPTP opening and closing via changes in CyP-D and other putative components such as ANT may answer these questions.

Summary and future directions

In conclusion, these results demonstrate that mPTP function regulates myocyte differentiation directly via redox signaling pathways and suggest that these changes in mPTP function, mitochondrial maturation, and ROS levels are a mechanism that protects the embryonic heart during a period of increasing energy demands but low oxygen supply. Therefore, these data may have clinical implications by suggesting that some cardiomyopathies and congenital heart defects may be due to disruption of myocyte differentiation secondary to defects in mPTP activity, mitochondrial maturation, and redox biology. Thus, not only does this research define the important role of mitochondrial maturation and redox state in the developing heart, but it also may lead to therapeutic innovations to promote mPTP closure or decrease oxidative stress to accelerate myocyte differentiation in cardiac development, cardiomyopathies, and cardiac regeneration. Finally, these data suggest that increased IMM permeability is physiologic in the developing heart and that CyP-D activity is a mechanism by which mPTP is regulated in the early heart. Future studies should determine the mechanisms that control mPTP activity in the developing myocyte and further characterize the redox signaling pathways that lie downstream of mitochondrial function to control myocyte differentiation in the developing heart.

EXPERIMENTAL PROCEDURES

Animals

All experiments were performed using wild type C57BL/6N mice or CyP-D null mice in a C57BL/6 background. Embryos were harvested at E9.5, 11.5, and 13.5 based on timed matings and on the morphology of the embryo.

Fluorescent imaging and analyses

Embryonic ventricles and outflow tracts were dissociated with papain and cultured in Dulbecco's modified Eagle's medium with fetal bovine serum and antibiotics (Polo-Parada et al., 2009). Live cultures were labeled with TMRE (20 nM), DCF (1 μM), MTG or MTR (200 nM), or calcein AM (1 μM) with cobalt chloride (1 μM). Fixed cultures were permeabilized and labeled with antibodies to AIF, cyt *c*, or α-actinin and fluorescent secondary antibodies. Images were taken using confocal and epifluorescence microscopes and analyzed using Image J or Image Pro 6 software.

Determination of mitochondrial structure and function

Analysis of mitochondrial length, aspect ratio (AR), form factor (FF), and area were quantified in live cells labeled with MTG (Hom et al, 2007; Quintanilla et al, 2009). $\Delta\psi_m$ was quantified as the ratio of TMRE to MTG intensity. Live cultures were loaded for 35 min with TMRE and MTG in Hepes-Tyrode's buffer, washed, and equilibrated for 20 minutes in the same buffer. ROS levels were measured by incubating cultures with DCF and MTR for 30 minutes in Krebs-Ringer-Hepes buffer supplemented with 5 mM glucose at 37°C, washed, and examined in the same buffer. ROS levels were expressed as average of fluorescence signal (F) minus background fluorescence (F0) (Quintanilla, 2009).

Determination of myocyte differentiation

Cultured myocytes were labeled with an anti-sarcomeric α-actinin antibody and analyzed as in Figure S3A to count the number of Z-bands per cell.

Electron microscopy

Pregnant dams were sacrificed by cervical dislocation and uterine segments were rapidly removed and dissected in EM fixative. Specimens were post-fixed in 1 % osmium tetroxide and embedded in EPON/Araldite resin. 70nm sections were stained with aqueous uranyl acetate and lead citrate. Sections were examined and photographed using a Hitachi 7650 TEM.

Western blot analysis

Homogenates of embryonic ventricles and outflow tracts were run on an SDS-polyacrylamide gel, transferred to nitrocellulose membranes, and probed with mouse anti-ANT1, CyP-D, and 75 kDa subunit of complex II.

Statistics

Statistical analyses were conducted using Prism or SAS System for Windows. Fluorescence data was analyzed using t-tests, ANOVA followed by Dunnett's post-hoc testing, or Kruskal-Wallis test with Dunn's post-hoc testing Mitochondrial ultrastructural classes were analyzed using a random effects model followed by pairwise comparisons using Tukey-Kramer adjustment. In all cases, a P value for significance was set at 0.05. All error bars represent S.E.M. unless otherwise noted.

For details of Experimental Procedures, please see the Supplemental Information.

Supplementary Material

Refer to Web version on PubMed Central for supplementary material.

Acknowledgments

We thank Paul Brookes, Robert Dirksen, and the members of the Mitochondrial Research and Innovation Group at the University of Rochester Medical Center for critical evaluation of this manuscript, Carmen Manella, David Mankus, Gayle Schneider for assistance with the electron microscope experiments, Cookie Wang for guidance with statistical methods, and Barbara Tisdale for technical support. This work was supported by Grants from the National Institutes of Health (R01HL093671 and RO1HL033333, S-S.S.), National Center for Research Resources (UL1 RR024160, G.A.P.), American Heart Association (G.A.P. and S-S.S.), and Children Cardiomyopathy Foundation (G.A.P).

REFERENCES

Aon MA, Cortassa S, O'Rourke B. Redox-optimized ROS balance: a unifying hypothesis. Biochim Biophys Acta. 2010; 1797:865–877. [PubMed: 20175987]

Baines CP, Kaiser RA, Purcell NH, Blair NS, Osinska H, Hambleton MA, Brunskill EW, Sayen MR, Gottlieb RA, Dorn GW, et al. Loss of cyclophilin D reveals a critical role for mitochondrial permeability transition in cell death. Nature. 2005; 434:658–662. [PubMed: 15800627]

Baines CP, Molkentin JD. Adenine nucleotide translocase-1 induces cardiomyocyte death through upregulation of the pro-apoptotic protein Bax. J Mol Cell Cardiol. 2009; 46:969–977. [PubMed: 19452617]

Basso E, Fante L, Fowlkes J, Petronilli V, Forte MA, Bernardi P. Properties of the permeability transition pore in mitochondria devoid of Cyclophilin D. J Biol Chem. 2005; 280:18558–18561. [PubMed: 15792954]

Borisov AB, Martynova MG, Russell MW. Early incorporation of obscurin into nascent sarcomeres: implication for myofibril assembly during cardiac myogenesis. Histochem Cell Biol. 2008; 129:463–478. [PubMed: 18219491]

Brookes PS, Yoon Y, Robotham JL, Anders MW, Sheu SS. Calcium, ATP, and ROS: a mitochondrial love-hate triangle. Am J Physiol Cell Physiol. 2004; 287:C817–C833. [PubMed: 15355853]

Buggisch M, Ateghang B, Ruhe C, Strobel C, Lange S, Wartenberg M, Sauer H. Stimulation of ES-cell-derived cardiomyogenesis and neonatal cardiac cell proliferation by reactive oxygen species and NADPH oxidase. J Cell Sci. 2007; 120:885–894. [PubMed: 17298980]

Burelle Y, Khairallah M, Ascah A, Allen BG, Deschepper CF, Petrof BJ, Des Rosiers C. Alterations in mitochondrial function as a harbinger of cardiomyopathy: lessons from the dystrophic heart. J Mol Cell Cardiol. 2010; 48:310–321. [PubMed: 19769982]

Chung S, Dzeja PP, Faustino RS, Perez-Terzic C, Behfar A, Terzic A. Mitochondrial oxidative metabolism is required for the cardiac differentiation of stem cells. Nat Clin Pract Cardiovasc Med. 2007; (4 Suppl 1):S60–S67. [PubMed: 17230217]

Conway SJ, Kruzynska-Frejtag A, Kneer PL, Machnicki M, Koushik SV. What cardiovascular defect does my prenatal mouse mutant have, and why? Genesis. 2003; 35:1–21. [PubMed: 12481294]

Crompton M. The mitochondrial permeability transition pore and its role in cell death. Biochem J. 1999; 341(Pt 2):233–249. [PubMed: 10393078]

De Palma C, Falcone S, Pisoni S, Cipolat S, Panzeri C, Pambianco S, Pisconti A, Allevi R, Bassi MT, Cossu G, et al. Nitric oxide inhibition of Drp1-mediated mitochondrial fission is critical for myogenic differentiation. Cell Death Differ. 2010; 17:1684–1696. [PubMed: 20467441]

Dumollard R, Carroll J, Duchen MR, Campbell K, Swann K. Mitochondrial function and redox state in mammalian embryos. Semin Cell Dev Biol. 2009; 20:346–353. [PubMed: 19530278]

Elrod JW, Wong R, Mishra S, Vagnozzi RJ, Sakthievel B, Goonasekera SA, Karch J, Gabel S, Farber J, Force T, et al. Cyclophilin D controls mitochondrial pore-dependent Ca2+ exchange, metabolic flexibility, and propensity for heart failure in mice. J Clin Invest. 2010; 120:3680–3687. [PubMed: 20890047]

Fontaine E, Eriksson O, Ichas F, Bernardi P. Regulation of the permeability transition pore in skeletal muscle mitochondria. Modulation By electron flow through the respiratory chain complex i. J Biol Chem. 1998; 273:12662–12668. [PubMed: 9575229]

Friberg H, Ferrand-Drake M, Bengtsson F, Halestrap A, Wieloch T. Cyclosporin A, but not fk506, protects mitochondria and neurons against hypoglycemic damage and implicates the mitochondrial permeability transition in cell death. J Neurosci. 1998; 18:5151–5159. [PubMed: 9651198]

Gunter TE, Sheu SS. Characteristics and possible functions of mitochondrial Ca(2+) transport mechanisms. Biochim Biophys Acta. 2009; 1787:1291–1308. [PubMed: 19161975]

Halestrap AP. What is the mitochondrial permeability transition pore? J Mol Cell Cardiol. 2009; 46:821–831. [PubMed: 19265700]

Hausenloy DJ, Lim SY, Ong SG, Davidson SM, Yellon DM. Mitochondrial cyclophilin-D as a critical mediator of ischaemic preconditioning. Cardiovasc Res. 2010; 88:67–74. [PubMed: 20400621]

Hom JR, Gewandter JS, Michael L, Sheu SS, Yoon Y. Thapsigargin induces biphasic fragmentation of mitochondria through calcium-mediated mitochondrial fission and apoptosis. J Cell Physiol. 2007; 212:498–508. [PubMed: 17443673]

Ingraham CA, Burwell LS, Skalska J, Brookes PS, Howell RL, Sheu SS, Pinkert CA. NDUFS4: creation of a mouse model mimicking a Complex I disorder. Mitochondrion. 2009; 9:204–210. [PubMed: 19460290]

Krishnan J, Ahuja P, Bodenmann S, Knapik D, Perriard E, Krek W, Perriard JC. Essential role of developmentally activated hypoxia-inducible factor 1alpha for cardiac morphogenesis and function. Circ Res. 2008; 103:1139–1146. [PubMed: 18849322]

Larsson NG, Wang J, Wilhelmsson H, Oldfors A, Rustin P, Lewandoski M, Barsh GS, Clayton DA. Mitochondrial transcription factor A is necessary for mtDNA maintenance and embryogenesis in mice. Nat Genet. 1998; 18:231–236. [PubMed: 9500544]

Lemasters JJ, Theruvath TP, Zhong Z, Nieminen AL. Mitochondrial calcium and the permeability transition in cell death. Biochim Biophys Acta. 2009; 1787:1395–1401. [PubMed: 19576166]

Mannella CA. Structure and dynamics of the mitochondrial inner membrane cristae. Biochim Biophys Acta. 2006; 1763:542–548. [PubMed: 16730811]

Nakagawa T, Shimizu S, Watanabe T, Yamaguchi O, Otsu K, Yamagata H, Inohara H, Kubo T, Tsujimoto Y. Cyclophilin D-dependent mitochondrial permeability transition regulates some necrotic but not apoptotic cell death. Nature. 2005; 434:652–658. [PubMed: 15800626]

Petronilli V, Miotto G, Canton M, Brini M, Colonna R, Bernardi P, Di Lisa F. Transient and long-lasting openings of the mitochondrial permeability transition pore can be monitored directly in intact cells by changes in mitochondrial calcein fluorescence. Biophys J. 1999; 76:725–734. [PubMed: 9929477]

Poelmann RE, Molin D, Wisse LJ, Gittenberger-de Groot AC. Apoptosis in cardiac development. Cell Tissue Res. 2000; 301:43–52. [PubMed: 10928280]

Polo-Parada L, Zhang X, Modgi A. Cardiac cushions modulate action potential phenotype during heart development [corrected]. Dev Dyn. 2009; 238:611–623. [PubMed: 19235920]

Porter GA Jr, Hom JR, Hoffman DL, Quintanilla RA, Bentley KLdM, Sheu S-S. Bioenergetics, mitochondria, and cardiac differentation. Prog Pediatr Cardiol. 2011; 31:75–81. [PubMed: 21603067]

Quintanilla RA, Jin YN, Fuenzalida K, Bronfman M, Johnson GV. Rosiglitazone treatment prevents mitochondrial dysfunction in mutant huntingtin-expressing cells: possible role of peroxisome proliferator-activated receptor-gamma (PPARgamma) in the pathogenesis of Huntington disease. J Biol Chem. 2008; 283:25628–25637. [PubMed: 18640979]

Quintanilla RA, Matthews-Roberson TA, Dolan PJ, Johnson GV. Caspase-cleaved tau expression induces mitochondrial dysfunction in immortalized cortical neurons: implications for the pathogenesis of Alzheimer disease. J Biol Chem. 2009; 284:18754–18766. [PubMed: 19389700]

Shepard TH, Muffley LA, Smith LT. Ultrastructural study of mitochondria and their cristae in embryonic rats and primate (N. nemistrina). Anat Rec. 1998; 252:383–392. [PubMed: 9811216]

Skulachev VP. Mitochondrial filaments and clusters as intracellular power-transmitting cables. Trends Biochem Sci. 2001; 26:23–29. [PubMed: 11165513]

Tampo Y, Kotamraju S, Chitambar CR, Kalivendi SV, Keszler A, Joseph J, Kalyanaraman B. Oxidative stress-induced iron signaling is responsible for peroxide-dependent oxidation of dichlorodihydrofluorescein in endothelial cells: role of transferrin receptor-dependent iron uptake in apoptosis. Circ Res. 2003; 92:56–63. [PubMed: 12522121]

Wang W, Fang H, Groom L, Cheng A, Zhang W, Liu J, Wang X, Li K, Han P, Zheng M, et al. Superoxide flashes in single mitochondria. Cell. 2008; 134:279–290. [PubMed: 18662543]

Yan P, Nagasawa A, Uosaki H, Sugimoto A, Yamamizu K, Teranishi M, Matsuda H, Matsuoka S, Ikeda T, Komeda M, et al. Cyclosporin-A potently induces highly cardiogenic progenitors from embryonic stem cells. Biochem Biophys Res Commun. 2009; 379:115–120. [PubMed: 19094963]

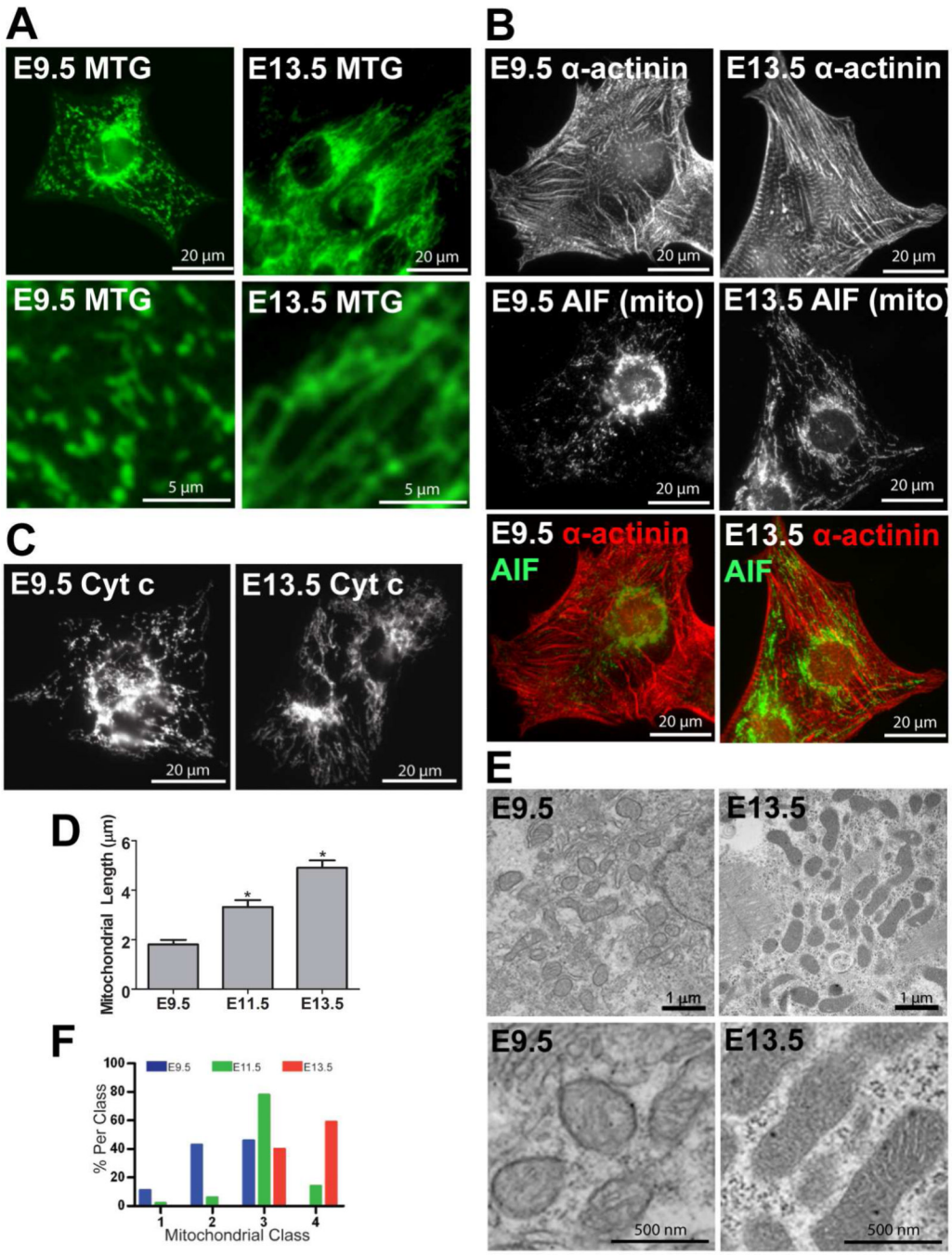

Figure 1. Mitochondrial morphology changes during cardiac development

(A) Epifluorescence microscopy of MTG in live cultured ventricular myocytes at ages E9.5 and 13.5. (B) Fixed myocytes stained for α-actinin in the contractile apparatus and AIF in mitochondria. (C) Fixed myocytes stained for cyt *c* in mitochondria. (D) Measurements of mitochondrial length in cultured WT E9.5, 11.5, and 13.5 myocytes (*P<0.05 compared to E9.5). (E) Transmission electron micrographs from WT E9.5 and 13.5 hearts. (F) A histogram of mitochondrial ultrastructure classes from electron micrographs from ventricular myocytes of WT E9.5, 11.5, 13.5 hearts. The weighted classifications were significantly different among the three ages (P<0.05).

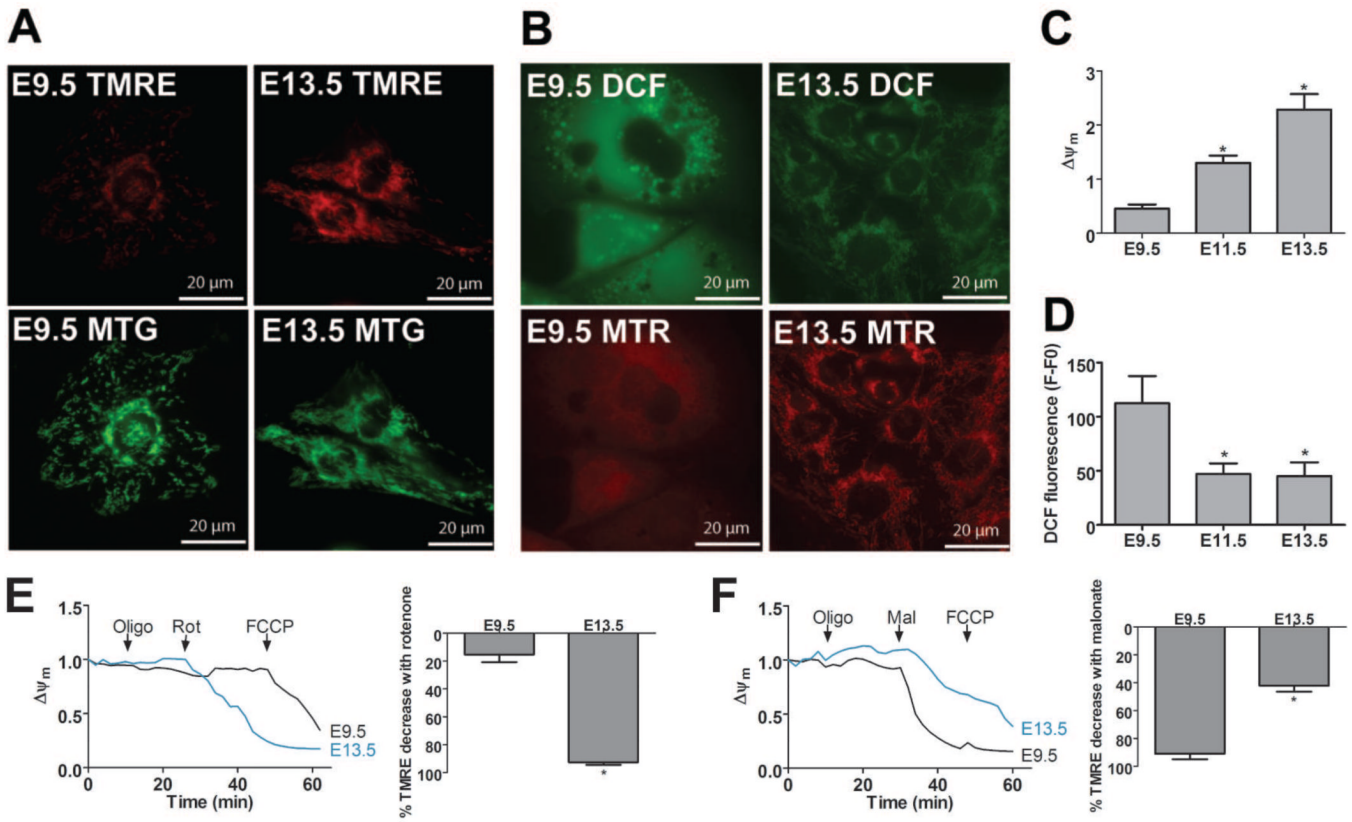

Figure 2. Mitochondrial function changes as the embryonic heart ages

(A and B) Epifluorescence microscopy of TMRE with MTG (A) and DCF with MTR (B) in cultured myocytes at E9.5 and 13.5. (C and D) Measurements of $\Delta\psi_m$ (C, TMRE normalized to MTG) and ROS (D, DCF fluorescence) in cultured E9.5, 11.5, and 13.5 myocytes (*P<0.05 compared to E9.5). (E and F) Representative traces of $\Delta\psi_m$ in myocytes treated with 1 μg/mL oligomycin (oligo), then either 1 μM rotenone (rot, E) or 2 mM malonate (mal, F) followed by 1 μM FCCP. Data is shown as ratio of fluorescence at any time point to first time point. Bar graphs represent the % change in TMRE after addition of rotenone or malonate compared to the total change after addition of the protonophore, FCCP (*P<0.05 compared to E9.5).

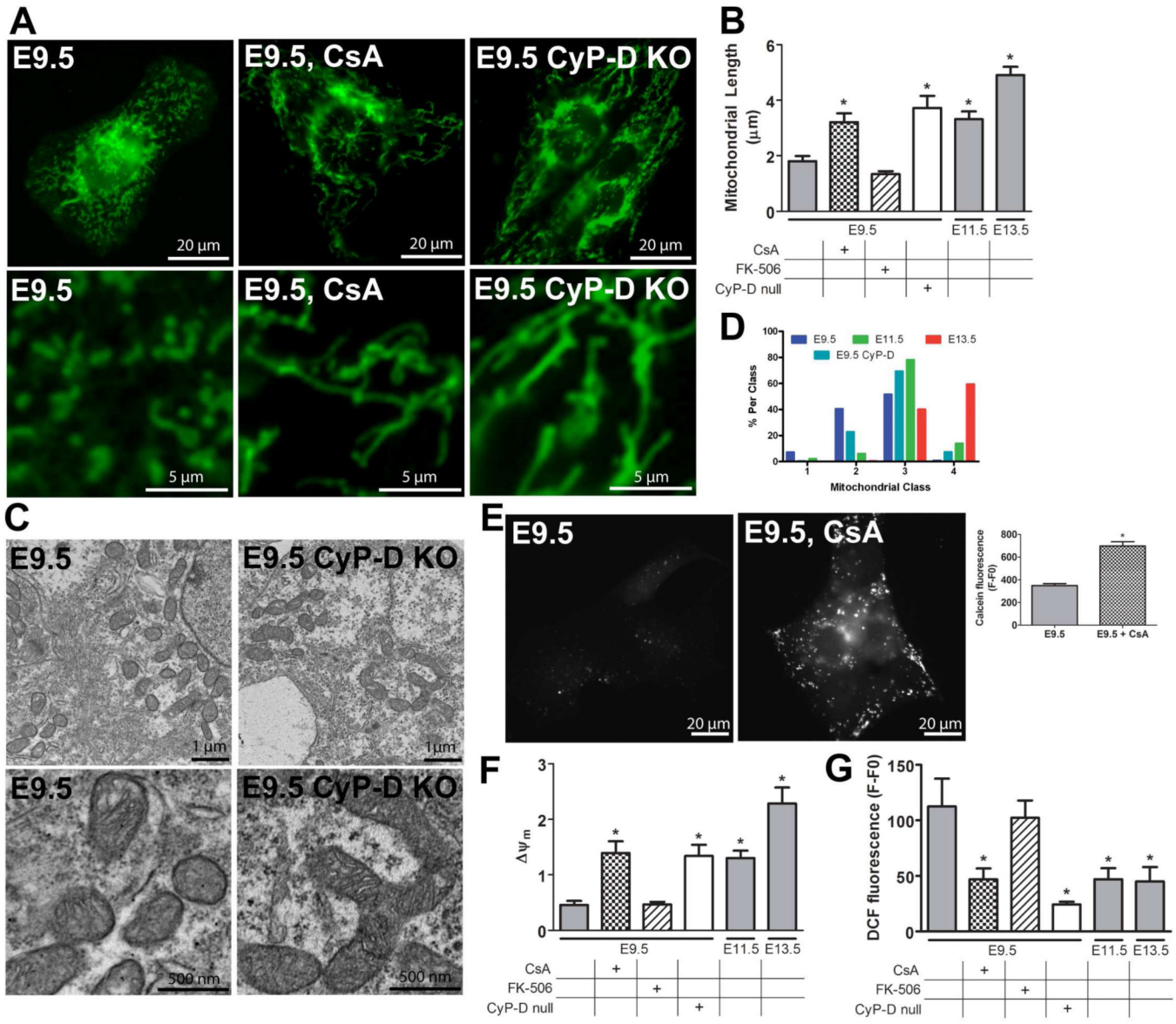

Figure 3. Mitochondrial structure and function changes after closure of the mPTP

(A) Epifluorescence microscopy of MTG in live E9.5 cultured ventricular myocytes: WT, WT with 500 nM Cyclosporin A (CsA) for 2 hours, and CyP-D null (CyP-D KO) myocytes. (B) Mitochondrial length in cultured WT E9.5 myocytes with and without treatment with 500 nM CsA or 500 nM FK-506 for 2 hours, CyP-D null E9.5 myocytes, and WT E11.5 and 13.5 myocytes (*P<0.05 compared to WT E9.5). (C) Electron micrographs of WT E9.5 and CyP-D null E9.5 hearts. (D) A histogram of mitochondrial ultrastructure classes in electron micrographs from ventricular myocytes of WT E9.5, 11.5, 13.5, or CyP-D null E9.5 hearts. (E) Images of E9.5 cultured ventricular myocytes stained with calcein-AM in the presence of $CoCl_2$. Quantification showed increased calcein fluorescence after treatment with 500 nM CsA (*P<0.05). (F and G) Measurements of $\Delta\psi_m$ (F) and ROS (G) in cultured WT E9.5 myocytes with and without treatment with 500 nM CsA or 500 nM FK-506 for 2 hours, CyP-D null E9.5 myocytes, and WT E11.5 and 13.5 myocytes (*P<0.05 compared to WT E9.5). Expanded graphical data is provided in Figure S2C–E.

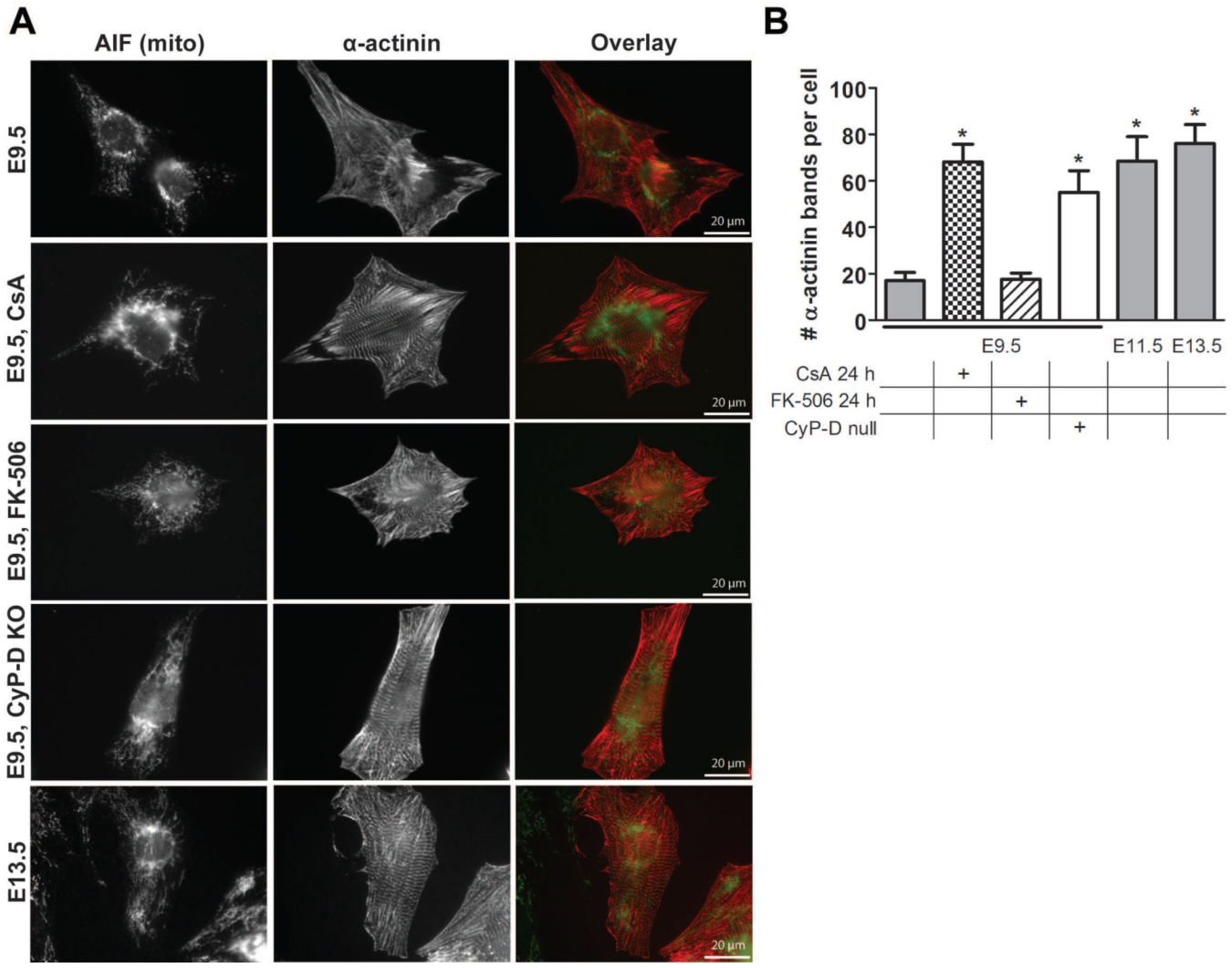

Figure 4. Closure of the embryonic mPTP enhances myocyte differentiation

(A) Cultured WT E9.5 myocytes with and without treatment with 500 nM CsA or 500 nM FK-506 for 2 hours, CyP-D null (KO) E9.5 myocytes, and WT E13.5 myocytes were stained with antibodies to α-actinin and AIF to label Z-bands and mitochondria, respectively. (B) Quantification of Z-band number in WT E9.5 myocytes with and without treatment with 500 nM CsA or 500 nM FK-506 for 2 hours, CyP-D null E9.5 myocytes, and WT E11.5 and 13.5 myocytes ($P<0.05$ compared to WT E9.5). Expanded graphical data and details of quantification are provided in Figures S2F and S3A.

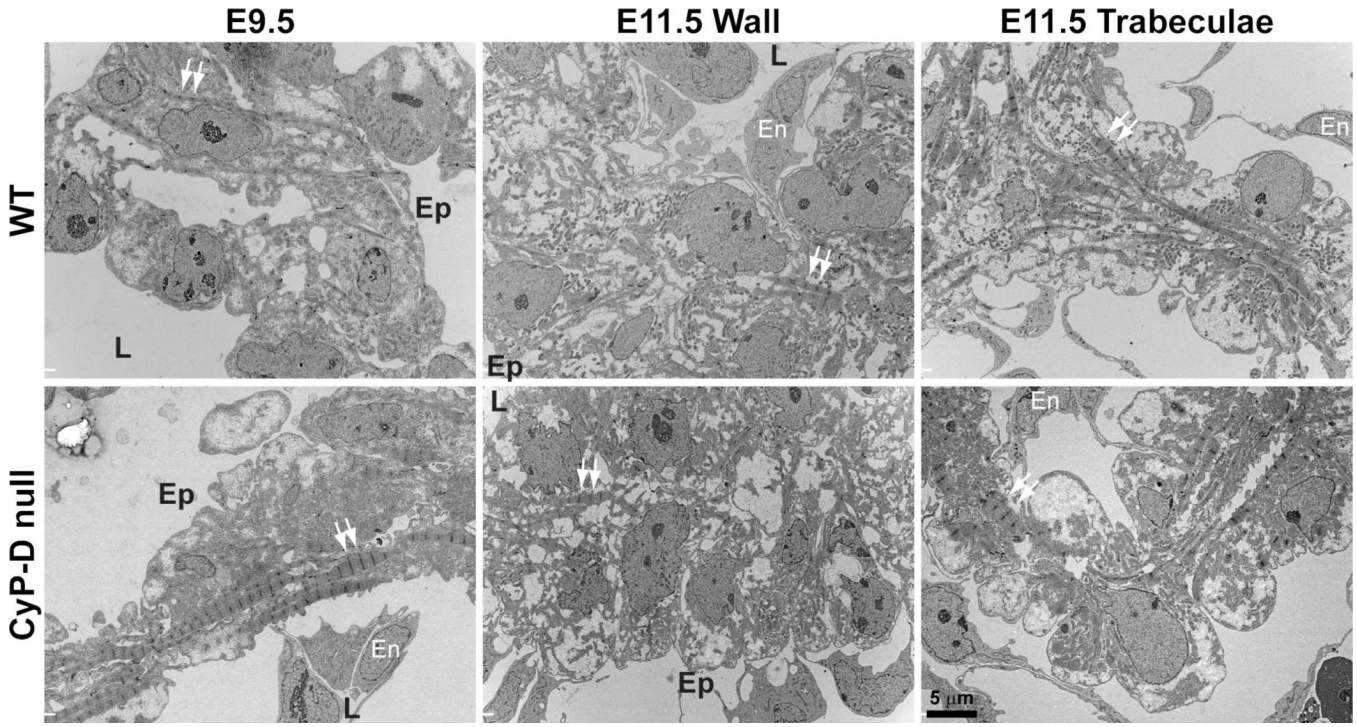

Figure 5. CyP-D deletion accelerates myocyte differentiation of E9.5, but not E11.5, myocytes *in vivo*

Images (3,500 × magnification) taken of the left ventricular wall of E9.5 (25–26 somites) and E11.5 hearts and trabeculae of E11.5 hearts from WT and CyP-D null embryos. Arrows: examples of Z-bands of the myofibrils; En: endothelial cell; L: lumenal side of the wall; Ep: epicardial surface.

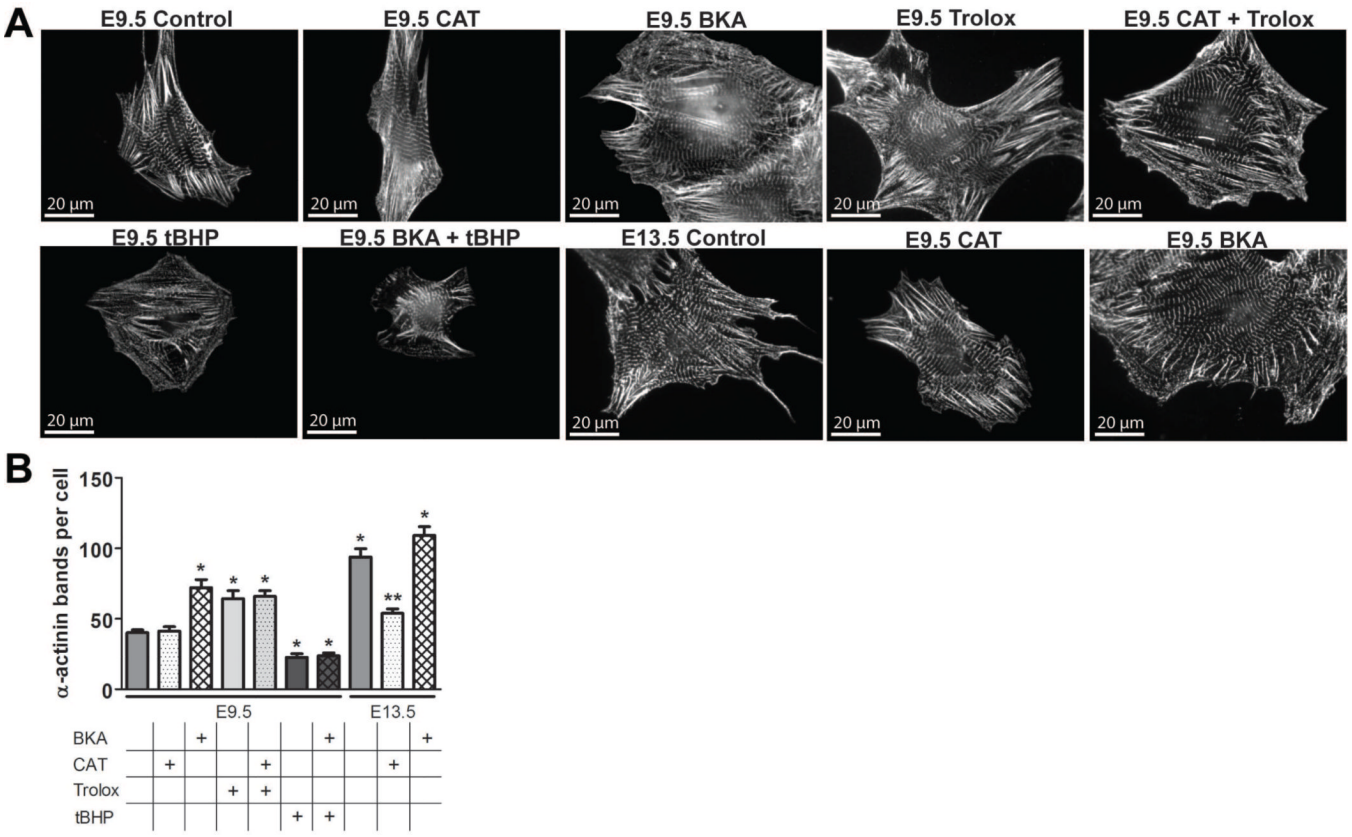

Figure 6. Myocyte differentiation is regulated by changes in oxidative stress downstream of mPTP activity

(A) Cultured WT E9.5 and 13.5 myocytes were treated with 100 μM bongkrekic acid (BKA), 100 μM carboxyatractyloside (CAT), 100 μM 6-Hydroxy-2,5,7,8-tetramethylchroman-2-carboxylic acid (Trolox), or 10 μM *tert*-butyl hydroperoxide (tBHP) from 24–48 hours in culture and stained with antibodies to α-actinin to label Z-bands. (B) Quantification of Z-band number in WT E9.5 and 13.5 myocytes treated with combinations of BKA, CAT, Trolox, or tBHP from 24–48 hours in culture ($P<0.05$ compared to WT *E9.5 or **E13.5).